Available online at www.sciencedirect.com
ScienceDirect
Catalysis Today 137 (2008) 385–389
CATALYSIS TODAY
www.elsevier.com/locate/cattod

Catalytic reduction of nitrous oxide with carbon monoxide over calcined Co–Mn–Al hydrotalcite

K. Pacultová [a,*], L. Obalová [a], F. Kovanda [b], K. Jirátová [c]

[a] *Technical University of Ostrava, 17. listopadu 15, Ostrava, Czech Republic*
[b] *Institute of Chemical Technology, Prague, Technická 5, Prague, Czech Republic*
[c] *Institute of Chemical Process Fundamentals CAS, Rozvojová 135, Prague, Czech Republic*

Available online 22 January 2008

Abstract

The N_2O catalytic reduction by carbon monoxide over Co–Mn–Al calcined hydrotalcite was studied. The effect of oxygen and that of CO/N_2O molar ratio on the rate of N_2O decomposition was examined. CO strongly enhanced N_2O conversion when O_2 was absent in the feed gas. In the presence of oxygen, carbon monoxide acts as a non-selective reductant thereby inhibiting N_2O destruction. Continuing excess of CO over N_2O without presence of O_2 led to a very slow reduction of the catalyst, which caused noticeable N_2O conversion decrease with progressing catalyst reduction. The simultaneous reduction of N_2O by CO and direct N_2O decomposition took place when CO was limiting reactant ($CO/N_2O < 1$) but only at temperatures, at which the direct decomposition is possible without presence of reductant. Simple reduction was observed when reactants ratio was $CO/N_2O \geq 1$.

Keywords: Nitrous oxide; Carbon monoxide; Catalytic reduction; Layered double hydroxides; Mixed oxide catalysts

1. Introduction

The simplest way to remove N_2O emissions from chemical industry is its decomposition to N_2 and O_2 (Eq. (1)). The catalytic N_2O decomposition over oxide catalysts (Fig. 1) can be described as an adsorption followed by oxidation of active sites (Eq. (2)) and subsequent removal of the deposited oxygen (Eqs. (3) and (4)). It is widely accepted that desorption of oxygen is the rate limiting step in N_2O decomposition [1]. Desorption of oxygen by recombination of two surface oxygen atoms (Eq. (3)) is negligible over some of tested catalysts and the main route of the surface oxygen removal is described by Eq. (4) [2]. Inhibition of reaction rate by oxygen could be caused by dissociative (backwards reaction (3)) or molecular adsorption of O_2 (Eq. (5)). The surface oxygen could be removed more easily in the presence of a reducing agent, e.g. light hydrocarbons [3], NH_3 [4], CO [5,6] and H_2 [7].

$$N_2O \xrightarrow{k_1} N_2 + O_2 \quad (1)$$

$$N_2O + CO \xrightarrow{k_6} N_2 + CO_2 \quad (6)$$

N_2O reduction by CO (Eq. (6)) can be utilized for lowering of N_2O emissions especially in processes where CO is already present in the waste gas (e.g. the oxalic acid production). Several different mechanisms of N_2O reduction with CO were proposed (Fig. 2). The most often published mechanism is ''redox'', when surface is oxidized by N_2O and consequently reduced by CO with simultaneous formation of CO_2. The ''redox'' reaction could proceed by two ways: adsorbed oxygen can react with adsorbed CO (Eqs. (2), (7) and (8)) [8] or with CO from gas phase according to Eley–Rideal mechanism (Eqs. (2) and (9)) [9,10]. The redox mechanism was published over SnO_2 [8], Cu/Al_2O_3 [11], Pt/Al_2O_3 [12–14], Rh(1 1 1) [15], Rh/Al_2O_3 [16] and ZnO [17]. The other mechanism is called ''associative''. The simultaneous oxidation and reduction are considered and the reaction proceeds via species adsorbed on the catalyst surface. Reaction can proceed between both reactants in adsorbed form (Eqs. (7), (10) and (11)) [6] or between adsorbed CO and N_2O from the gas phase (Eqs. (7) and (12)) [5]. The associative mechanism was described over Rh/Al_2O_3 [6], Ag/Al_2O_3 [6] MgO [18,19], Co_3O_4 [5,20], NiO [21], MnO [20], $CuCo_2O_4$ [17] and Fe_2O_3/SiO_2 [22].

* Corresponding author. Tel.: +420 59 699 1531; fax: +420 59 732 3396.
E-mail address: katerina.pacultova@vsb.cz (K. Pacultová).

0920-5861/$ – see front matter © 2007 Elsevier B.V. All rights reserved.
doi:10.1016/j.cattod.2007.11.062

$$N_2O + * \xrightarrow{k_2} N_2 + O* \quad (2)$$
$$2\,O* \xleftrightarrow{K_3} O_2 + 2* \quad (3)$$
$$N_2O + O* \xrightarrow{k_4} N_2 + O_2 + * \quad (4)$$
$$O_2 + * \xrightarrow{k_5} O_2* \xrightarrow{*\,(fast)} 2\,O* \quad (5)$$

where * means active site, k means rate constant and K means equilibrium constant

Fig. 1. The sequence of elementary steps for catalytic decomposition of N_2O, k means rate constant and K means equilibrium constant.

In some cases both mechanisms take part in the reaction and their contribution to the overall reaction rate depends on the experimental conditions such as temperature [31], extent of catalyst reduction [31] or each mechanism take place at different active sites [5]. Combination of redox and associative mechanisms was considered over calcined hydrotalcites [9] and over Fe-silicalite [8]. Apart from simple reduction, the simultaneous reduction and direct N_2O decomposition can also proceed [32].

The reaction order with respect to CO (m) corresponding to rate law $r = k\,p_{CO}^{m}\,p_{N_2O}^{l}$ varied from negative (Rh [15], Rh/Al_2O_3 [16,23,24], Pt–Rh/Al_2O_3 [25], Pt/Al_2O_3 [14], Pd/oxid [26]) over zero (MoO_3/SiO_2 [27], NiO [21], Co_3O_4 [20]) to positive (MgO [18], Sc_2O_3 [18], ZnO [17], V_2O_5 [28], Fe zeolit [29], Au/TiO_2 [30]). The reaction order with respect to CO was temperature dependent—it changed from negative to positive with increasing temperature over Cu/Al_2O_3 [11], and changed from zero to positive over MnO [20].

Mixed oxides prepared by calcination of hydrotalcite-like precursors have been shown as active catalysts for direct N_2O decomposition [33]. The most active catalyst among all mixed oxides tested by our group was the Co–Mn–Al one [34]. In the present work, the effect of CO, O_2 and CO + O_2 mixture on the activity of this catalyst in N_2O decomposition is studied. The concentrations of CO and O_2 were chosen with respect to the real concentrations in waste gas from the oxalic acid production (0.1 mol% N_2O, 20 mol% O_2, 0.15 mol% CO).

2. Experimental

The Co–Mn–Al hydrotalcite-like precursor with Co:Mn:Al molar ratio of 4:1:1 was prepared by coprecipitation of nitrate solutions. The catalyst was obtained by precursor calcination at 500 °C. The details of catalyst preparation and characterization are described elsewhere [34].

Redox mechanism:

$$N_2O + * \xrightarrow{k_2} N_2 + O* \quad (2)$$
$$CO + * \xleftrightarrow{K_7} CO* \quad (7)$$
$$CO* + O* \xrightarrow{k_8} CO_2 + 2* \quad (8)$$
$$CO + O* \xrightarrow{k_9} CO_2 + * \quad (9)$$

Associative mechanism:

$$CO + * \xleftrightarrow{K_7} CO* \quad (7)$$
$$N_2O + * \xleftrightarrow{K_{10}} N_2O* \quad (10)$$
$$CO* + N_2O* \xrightarrow{k_{11}} CO_2 + N_2 + 2* \quad (11)$$
$$CO* + N_2O \xrightarrow{k_{12}} CO_2 + N_2 + * \quad (12)$$

Fig. 2. Elementary steps for catalytic reduction of N_2O by CO published in the literature.

The N_2O catalytic reaction was performed in a fixed-bed reactor in the temperature range 300–450 °C with the total flow rate 330 ml min^{-1} NTP (273 K, 101.325 Pa), 0.33 g of sample with particle size 0.160–0.315 mm and inlet concentration 0.1 mol% N_2O in the presence of CO (0.05–0.3 mol%) balanced by helium. The influence of oxygen (20 mol%) in the reaction mixture was also tested. The catalyst was activated in He for 1 h at overall flow rate of 50 ml/min and temperature 450 °C before first experimental run.

A gas chromatograph Agilent Technologies 6890N with TCD detector was used to analyze N_2O, CO, CO_2, O_2 and N_2. The valve system for switching the columns PORAPLOT Q 30 m × 0.53 mm × 40 μm for separating N_2O and CO_2 and MOLSIEVE 5A 30 m × 0.53 mm × 25 μm for separating CO, N_2 and O_2 was used. The analysis proceeded at 40 °C, the detector temperature was 200 °C, overall flow was kept at 3.5 ml/min and He was used as a carrier gas. The analysis lasted 7.5 min.

The calculated conversions in measurements, in which excess of CO without presence of oxygen was used, were calculated after first stabilizing of concentrations at the reactor outlet, minimally 1 h after change of conditions, but usually after much longer period. It was observed that first stabilizing of concentrations needs longer time with decreasing temperature. Moreover, in a view of long duration of the experiment (more than 10 h), subsequent slow decrease in N_2O conversion was observed. The subsequent slow decrease of conversion was attributed to the slow reduction of the catalyst; therefore defining the steady state conversion was almost impossible.

3. Results and discussion

Co–Mn–Al spinel was detected in the powder XRD pattern of the calcined sample. Surface area of catalyst determined by BET method was 92.7 $m^2\,g^{-1}$, main part of the surface was ascribed to mesopores (92 $m^2\,g^{-1}$). The details of catalyst characterization are described in [34].

Catalytic reduction of N_2O with CO in an inert gas and in the presence of O_2 is compared with direct N_2O decomposition in inert gas and in the presence of oxygen in Fig. 3. The direct N_2O decomposition is slightly inhibited by oxygen. CO strongly enhanced the N_2O conversion when O_2 was absent in the feed gas; 100% N_2O conversion was achieved already at 350 °C. However, in the presence of O_2, CO acted as a non-selective reductant in the catalytic reduction of N_2O and inhibited N_2O destruction. N_2O conversion is lower not only in comparison with N_2O reduction by CO but also even compared to direct decomposition in the presence of oxygen. Decrease in N_2O conversion in the presence of O_2 and CO was also reported by

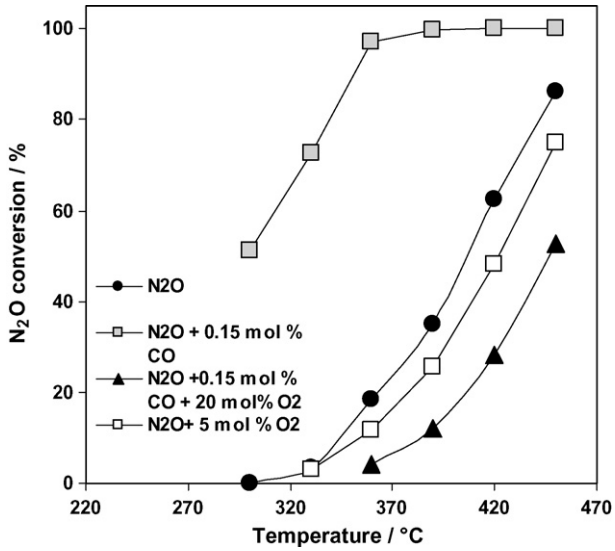

Fig. 3. Temperature dependence of N_2O conversion. *Conditions*: 0.1 mol% N_2O balanced by He, 330 ml/min, 0.33 g.

Chang et al. [9] over mixed oxide catalyst derived from hydrotalcite-like precursors and by Kapteijn et al. [35] over Cu/Cr oxide catalysts. Authors attributed the decrease in N_2O conversion to the dominant adsorption of oxygen, which inhibits the adsorption of N_2O and CO and the sequential reactions. However, the N_2O and CO conversions were not affected by the presence of O_2 on the Fe-ZSM-5, which confirms the selectivity of the reducing agent for N_2O [36].

The influence of CO/N_2O molar ratio in the reaction mixture on the N_2O conversion is demonstrated in Fig. 4. The N_2O conversion increased with increasing CO/N_2O molar ratio in the feed gas, reaching the maximum at stoichiometric consumption of CO (Eq. (6)). Subsequent course of N_2O conversion with increasing CO/N_2O molar ratio is temperature

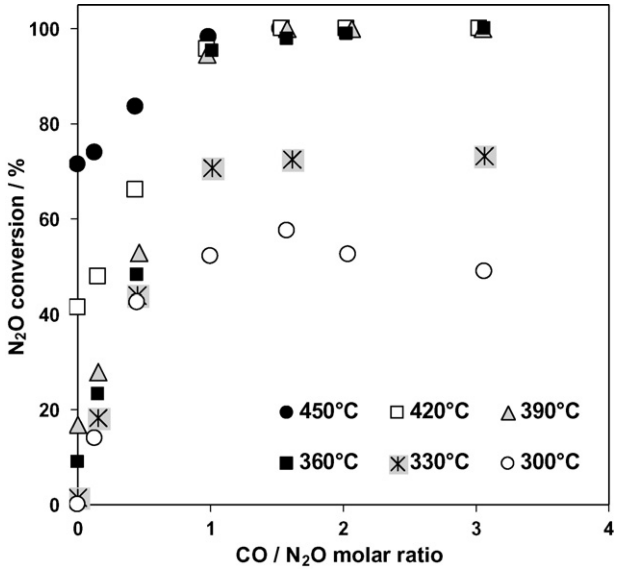

Fig. 4. Dependence of N_2O conversion on the CO/N_2O molar ratio. *Conditions*: 0.1 mol% N_2O + CO balanced by He, 330 ml/min, 0.33 g.

dependent. At higher temperatures (360–450 °C), constant 100% conversion of N_2O was achieved, at lower temperatures (300–330 °C), N_2O conversion was also constant, but lower than 100% and decreased with decreasing temperature. The rate of N_2O decomposition usually decreased with increasing amount of CO in the feed gas over catalysts based on Rh, Pt and Pd [26]. An inhibition of the N_2O decomposition by CO was explained by the strong adsorption of CO on the precious metals, which results in a considerable occupation of the available surface sites and suppression of N_2O adsorption and decomposition. Kapteijn et al. [37] described the different effect of CO amount on N_2O conversion over zeolites. While the N_2O conversion over Fe-ZSM-5 increased with increasing amount of CO at the reactor inlet, the N_2O conversion over Co-ZSM-5 increased only up to CO/N_2O molar ratio of 0.5, when the constant N_2O conversion was achieved. The enhancement by CO over Cu-ZSM-5 passed through a maximum as a function of CO pressure due to the strong adsorption at the reduced sites.

Apart from N_2 and CO_2, O_2 was also found in the reaction products in our measurements at temperatures 360–450 °C when N_2O was in the excess. The simultaneous reduction (Eq. (6)) and direct decomposition (Eq. (1)) took place when CO was limiting reactant ($CO/N_2O < 1$), but only at temperatures, at which the direct decomposition is possible without presence of reductant. Simple reduction was observed when reactants were dosed in the stoichiometric ratio or when the reductant was present in the excess ($CO/N_2O \geq 1$). No direct decomposition (Eq. (1)), occurring simultaneously with the interaction of CO with N_2O (Eq. (6)) during admission of stoichiometric pulses of N_2O and CO, was observed also over Co_3O_4 [5]. Over Fe-ZSM-5 the product distribution clearly showed the 1:1 stoichiometry for the reduction of N_2O and CO (Eq. (6)) at 673 K in the whole range of inlet molar ratio CO/N_2O from 0 to 2. However, some oxygen was still observed over Cu-ZSM-5 at low CO concentrations ($CO/N_2O < 1$); both reactions (Eqs. (1) and (6)) occurred simultaneously [37].

The temperature dependence of N_2O conversion for different CO/N_2O inlet molar ratios is shown in Fig. 5. The highest enhancement of N_2O conversion was achieved at low temperatures when CO was the limiting reactant ($CO/N_2O \leq 1$). The N_2O conversion profiles shifted gradually with increasing temperature to that of direct N_2O decomposition ($CO/N_2O = 0$). The same tendency of N_2O conversion profiles was observed over Fe-ZSM-5 [32]. The 100% CO conversion was always achieved when the CO was limiting reactant and simultaneous direct decomposition (O_2 was detected at the reactor outlet) and reduction of N_2O proceeded (360–450 °C) (not shown). Therefore it is supposed that the reduction is faster than the direct decomposition ($r_6 > r_1$). The reaction of N_2O and CO (Eq. (6)) presumably takes place at the beginning of the catalyst bed, contacting first with the gas mixture, while direct N_2O decomposition with subsequent O_2 production occurs after CO is consumed [32].

In order to understand the mechanism of N_2O + CO reaction over Co–Mn–Al mixed oxide catalyst, an interaction of CO with the catalyst and O_2 (without N_2O) was also tested. While

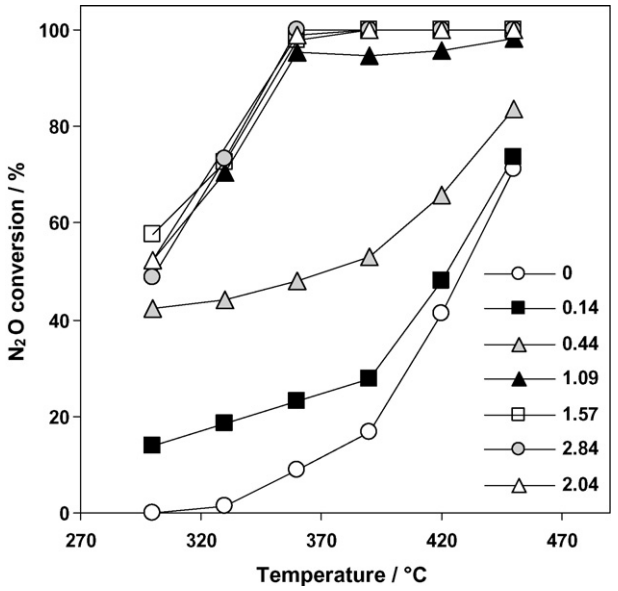

Fig. 5. Temperature dependence of N_2O conversion. *Conditions*: 0.1 mol% N_2O + CO balanced by He, 330 ml/min, 0.33 g, numbers in the legend mean CO/N_2O molar ratios in the feed gas.

the majority of CO reduced catalyst surface generating CO_2, a part of CO was accumulated on the catalyst surface, when only CO and He were present in the feed gas. When excess of O_2 was added to the CO inlet, CO reacts very easily with oxygen and 100% conversion of CO was reached in the examined temperature range of 300–450 °C. The homogenous reaction of CO + O_2 was found out to be negligible at given conditions. The detailed study of interaction of CO with the catalyst will be presented in the next paper [38].

The mechanism of N_2O + CO reaction can be described by Eqs. (2), (9), (7), (12), (4), (8) and (13) in Fig. 6. The rate of surface oxygen scavenging by N_2O (Eq. (4)) is slower than by CO (Eq. (9)) because no oxygen was observed at the outlet when N_2O was limiting reactant or N_2O and CO was dosed stoichiometrically. In this case, the main route for surface oxygen decrement is expressed by reaction (9) which can proceed in two steps (7) and (8) [6,9]. Both of reactions (4) and (9) can contribute to the oxygen consumption when N_2O is in the excess. The reaction (12) can contribute to the overall process only if the adsorption of CO (Eq. (7)) occurs at given conditions. When N_2O is limiting reactant, reaction (13) also takes place—continuing excess of CO over N_2O led to a very slow reduction of the catalyst. Overall consumption of N_2O is

$$N_2O + * \xrightarrow{k_2} N_2 + O^* \quad (2)$$
$$CO + O^* \xrightarrow{k_9} CO_2 + * \quad (9)$$
$$CO + * \xleftrightarrow{K_7} CO^* \quad (7)$$
$$CO^* + N_2O \xrightarrow{k_{12}} CO_2 + N_2 + * \quad (12)$$
$$N_2O + O^* \xrightarrow{k_4} N_2 + O_2 + * \quad (4)$$
$$CO^* + O^* \xrightarrow{k_8} CO_2 + 2* \quad (8)$$
$$CO + O^{\#} \xrightarrow{k_{13}} CO_2 + \# \quad (13)$$

where # means subsurface active site

Fig. 6. Proposed sequence of elementary steps for catalytic reduction of N_2O by CO.

given by reactions (2), (12) and (4). Contributions of individual reactions to the overall rate of N_2O destruction depend on the used experimental conditions.

The addition of oxygen to the N_2O + CO mixture caused a decrease in N_2O conversion (Fig. 3). Similarly as mentioned above, reactions (2) (4) and (12) are considered as routes of N_2O consumption. We suppose that in the presence of high amount of oxygen, the catalyst surface is primarily covered by adsorbed oxygen and/or CO. Catalytic reaction between CO and oxygen resulting in CO_2 formation is much faster than the rates of reactions (12) and (4), as was proposed in the literature [14,16] and also confirmed by our experiments. Thus, decrease of N_2O consumption rate in the presence of CO and O_2 could be caused by lowering of amount of surface reactive species (O* and CO*) and active sites (*) necessary for reactions (12), (4) and (2) by reactions (3), (7) and (9).

Apart from reactions given above, an accumulation of CO on the catalyst during reaction also took place as it was confirmed by analysis of fresh and used catalyst. The IR spectra showed a clear evidence of increased amount of carbonate species, probably in monodentate coordination. The increase in carbon content was also confirmed by analysis of total carbon however, the role of carbonate species in proposed mechanisms is still unclear.

It is obvious that N_2O + CO reaction over mixed metal oxide catalyst is very complex and exact elucidation of reaction mechanism is very difficult. More insights into this mechanism could be acquired by experiments with isotopically labeled molecules, in situ FTIR measurements or providing transient pulse experiments.

4. Conclusions

CO strongly enhanced N_2O conversion when O_2 was absent in the feed gas—100% N_2O conversion was achieved at 350 °C. In the presence of oxygen, carbon monoxide acts as a non-selective reductant in the catalytic reduction of N_2O over studied catalyst thereby inhibiting N_2O destruction. Continuing excess of CO over N_2O led to a very slow reduction of the catalyst, which caused noticeable N_2O conversion decrease with progressing catalyst reduction. If the time delay is long enough, the destruction of the catalyst structure can occur. From the practical point of view such a situation cannot occur because outgases usually contain excess of oxygen. On the other hand, the presence of oxygen causes a decrease in catalyst activity for N_2O abatement in comparison with reduction of N_2O with CO without O_2 and also with direct N_2O decomposition. In spite of the negative effect of O_2 in the presence of CO, the Co–Mn–Al mixed oxide catalyst prepared by calcination of hydrotalcite-like precursor represents the active catalyst suitable for application in N_2O abatement, however further tests in the presence of other typical effluents such as H_2O or NO_x are necessary.

Acknowledgement

This work was supported by the Czech Science Foundation (project 106/05/0366) and by the Ministry of Education, Youth

and Sports of the Czech Republic (research projects 6046137302 and NPV II 2B06068). We thank Nanotechnology Centre of Technical University of Ostrava for IR, XRD and TC analysis.

References

[1] F. Kapteijn, J.R. Mirasol, J.A. Moulijn, Appl. Catal. B 9 (1996) 25.
[2] L. Obalová, V. Fíla, Appl. Catal. B 70 (2007) 353.
[3] N.W. Cant, D.C. Chambers, Y. Yoshinaga, Catal. Commun. 5 (2004) 625.
[4] A.G. Vargas, G. Delahay, B. Coq, Appl. Catal. B 42 (2003) 369.
[5] R. Sundararajan, V. Srinivasan, Appl. Catal. A 141 (1996) 45.
[6] T.N. Angelidis, V. Tzitzios, Appl. Catal. B 41 (2003) 357.
[7] G. Delahay, M. Mauvezin, A.G. Vargas, B. Coq, Catal. Commun. 3 (2002) 385.
[8] J. Pérez-Ramírez, E.V. Kondratenko, M.N. Debbagh, J. Catal. 233 (2005) 442.
[9] K.S. Chang, H.J. Lee, Y.S. Park, J.W. Woo, Appl. Catal. A 309 (2006) 129.
[10] M.N. Debbagh, A.B. Bueno-López, C.S. Martinéz, J. Pérez-Ramírez, Appl. Catal. A 327 (2007) 66.
[11] A. Dandekar, M.A. Vannice, Appl. Catal. B 22 (1999) 179.
[12] R.R. Sadhankar, J. Ye, D.T. Lynch, J. Catal. 146 (1994) 511.
[13] R.S. Sadhankar, D.T. Lynch, J. Catal. 149 (1994) 278.
[14] P. Granger, P. Malfoy, P. Esteves, L. Leclerq, G. Leclerq?, J. Catal. 187 (1999) 321.
[15] D.N. Belton, S.J. Schmieg, J. Catal. 138 (1992) 70.
[16] R. McCabe, C.H. Wong, J. Catal. 121 (1990) 4221.
[17] K. Tanaka, G. Blyholder, J. Phys. Chem. 76 (1972) 1807.
[18] B.W. Krupay, R.A. Ross, Can. J. Chem. 56 (1978) 24476.
[19] B. Hori, N. Takezawa, Catal. Lett. 12 (1992) 383.
[20] B.W. Krupay, R.A. Ross, Can. J. Chem. 56 (1978) 10.
[21] B.W. Krupay, R.A. Ross, Z. Phys. Chem., Neue Folge 106 (1977) 83.
[22] H. Randal, R. Doepper, A. Renken, Can. J. Chem. Eng. 74 (1996) 586.
[23] L. Chmielarz, P. Kustrowski, M. Kruszec, R.J. Dziembaj, Porous Mater. 12 (2005) 1836.
[24] D.O. Uner, J. Catal. 178 (1998) 382.
[25] P. Granger, P. Malfoy, G. Leclerq, J. Catal. 223 (2004) 142.
[26] J.H. Holles, M.A. Switzer, R.J. Davis, J. Catal. 190 (2000) 247.
[27] A. Kazusaka, J.H. Lunsford, J. Catal. 45 (1976) 25.
[28] B.W. Krupay, R.A. Ross, J. Catal. 50 (1977) 220.
[29] L. Kiwi-Minsker, D.A. Bulushev, A. Renken, J. Catal. 219 (2003) 273.
[30] N.W. Cant, N.J. Ossipoff, Catal. Today 36 (1997) 125.
[31] B. Hori, N. Takezawa, H. Kobayashi, J. Catal. 80 (1983) 437.
[32] M.N.D. Boutarbouch, J.M.G. Cortés, M. Begrani, C.S. Martinéz, J. Peréz-Ramírez, Appl. Catal. B 54 (2004) 115.
[33] S. Kannan, Appl. Clay Sci. 13 (1998) 347.
[34] L. Obalová, K. Jirátová, F. Kovanda, K. Pacultová, Z. Lacný, Z. Mikulová, Appl. Catal. B 60 (2005) 289.
[35] F. Kapteijn, S. Stegenga, N.J.J. Dekker, J.W. Bijsterbosch, J.A. Moulijn, Catal. Today 16 (1993) 273.
[36] M.N. Debbagh, C.S. Martinéz, J. Pérez-Ramírez, Appl. Catal. B 70 (2007) 335.
[37] F. Kapteijn, G. Marbán, J.R. Mirasol, J.A. Moulijn, J. Catal. 167 (1997) 256.
[38] K. Pacultová, to be published.